On the combination of a linear field free trap with a time-of-flight mass spectrometer

Alfonz Luca,[a] Stephan Schlemmer, Ivo Čermák, and Dieter Gerlich
University of Technology, Chemnitz, Institute of Physics, 09107 Chemnitz, Germany

A new instrument has been developed which combines a rf ring electrode trap and a time-of-flight mass spectrometer (TOF-MS). The wide field free storage volume of such a trap enables the study of low temperature ion-molecule collisions; however it is not straightforward to match the nonlocalized ion cloud to the TOF-MS. For obtaining sufficient mass resolution, a special pulse sequence has been developed to transfer the ions from the whole trap volume to a small region in the vicinity of the exit electrode. Additional compression is achieved via buffer gas relaxation prior to extracting the ions. Using a linear flight path of 57 cm, a mass resolution of about 50 is routinely achieved. The mass range of the whole instrument, which is determined by the operating conditions both of the trap and the TOF-MS, has been estimated to be 3–700 u. The actual characteristics of the instrument such as mass range, resolution, and dynamical range have been determined and the results have been analyzed. As a typical application of the new instrument, the growth of $(CO)_n^+$ cluster ions is investigated at 80 K. The simultaneous detection of all masses of interest as a function of storage time allows one to follow in detail the kinetics of the reaction and loss processes involved. Limitations of the method are discussed together with ways to overcome them in an improved setup. © *2001 American Institute of Physics.* [DOI: 10.1063/1.1373666]

I. INTRODUCTION

The basic principle of time-of-flight (TOF) mass spectrometry resides in the fact that ions with different mass to charge ratio have well separated flight times if they start with suitable initial conditions in an adequate field geometry. Using today's fast and sensitive ion detectors high mass range, good resolution and large dynamical range are typical benefits of this mass analyzing technique.[1–3] TOF analysis is especially easy to adapt in photoionization experiments where ions can be formed by very short and strongly focused light pulses. In general, however, the ions start at different times in different places and often with different initial velocities, affecting the overall mass resolution. In the last decades, various methods have been invented to reduce the influence of spread in initial conditions. In principle one has to find the best transformation of the initial phase space volume to the acceptance of the detector; some related theoretical considerations can be found in Refs. 4 and 5. In practice, improvements are based on proper spatial and/or temporal arrangement of electrical fields. For example, spatial focusing conditions for linear TOF arrangements are given in Refs. 1 and 6. For reducing the influence of an energy distribution, electrostatic mirrors have been employed;[7] also multiple reflections have been tested.[8] Time dependent fields, sometimes called time-lag[1] and postacceleration,[9] can be used for a further improvement of the mass resolution.

One of the most important benefits of a time-of-flight mass spectrometer (TOF-MS) is the fact that a whole mass spectrum is obtained already with a single bunch of ions. In comparison to mass analysis by scanning devices, much measuring time can be saved, especially if a wide mass range is of interest. In addition, this feature makes the data analysis tolerant against intensity fluctuations. Each spectrum of a single bunch of ions can be normalized to the total number of detected ions reducing the statistical errors of the measurement. From a practical point of view, the mechanical design of a TOF-MS is rather simple; usually only a few electrodes are necessary for creating the appropriate electric fields. Also the electronics for data collection and acquisition are standard and today comparably inexpensive. This makes TOF-MS a popular method in many applications. The integration of this technique into a trapping experiment is the subject of the present study.

Trapping of ions is a powerful technique for studying ion-molecule interactions because storage time and target density can be varied over a large range, therefore enabling the study of fast as well as slow processes. Widely used are Penning or Paul traps for studying ion-molecule reactions at hyperthermal energies as well as fragmentation of ions induced by collisions or by laser light, see, e.g., Ref. 10. Less common are those rf traps which are characterized by a wide field free region. They are especially well suited for studying ion-molecule collisions at low temperatures. Details of the rf trapping technique and practical design considerations are discussed thoroughly in Ref. 11. Two special devices, the ring electrode trap (RET) and the 22-pole trap (22PT), have been used in our group for investigating a large variety of ion-molecule reactions at low collision energies. The high sensitivity of the method has been demonstrated particularly by detecting the very unlikely process of radiative association.[12] Other studies include the growth of weakly

[a]Electronic mail: luca@physik.tu-chemnitz.de

2900

bound hydrogen cluster ions[13] via ternary association and their deuteration[14] at 10 K, as well as laser induced reactions.[15,16] In all these applications, a conventional quadrupole mass spectrometer (QMS) has been used to analyze, mass by mass, the ion cloud. In the cluster experiments more than ten product channels had to be analyzed sequentially. In order to reduce the measuring time, simultaneous detection of a range of masses is required. From the various possible solutions, e.g., sequential mass selective ejection from the trap or the use of a magnetic sector field with a position sensitive detector, mass separation by TOF has been used in this work.

Several solutions for combining trapping and TOF-MS techniques have been reported in the literature. For example, coupling of rf quadrupole traps to TOF-MS was described in Refs. 17–19. Typically the mass resolution is on the order of several hundred with linear TOF, using a reflectron design, several thousand was achieved.[17] In the special case of a quadrupole trap, often named Paul trap, the harmonic effective potential confines the ion cloud in all three dimensions. This leads to a rather precise localization of the ions, especially with buffer gas cooling and, therefore, good starting conditions are created for TOF analysis. A problem, however, caused by the surrounding rf field is that the extraction has to take place at the proper rf phase or, alternatively, that the rf voltage has to be switched off, either suddenly or adiabatically. Also linear ion guides and traps have been connected to TOF devices, using a perpendicular TOF arrangement following extraction.[2,3,20]

The linear field geometry of the RET and the 22PT makes it easy to inject and extract ions via suitable gate electrodes. In addition, phase space compression via collisions with cold buffer gas leads to initial conditions superior to all other trapping devices. However, in these traps, the ions are distributed over a rather large spatial volume which requires either suitable compression steps prior to TOF analysis or other solutions. In order to perform tests in this direction, an existing trap apparatus has been modified. In the following, the experimental setup is described in detail, followed by a discussion of mass calibration, resolution, and dynamical range. Details of the compression phase in the RET are given. For illustration of the features of the device, the growth of $(CO)_n^+$ clusters is studied. In the last part, various ways to improve the present design and operational method are outlined.

II. EXPERIMENTAL SETUP

As mentioned above, the central element of the present apparatus is a rf ring electrode trap, constructed for studying ions in a low temperature environment. The typical mode of operation, which has been described in Ref. 21, is briefly summarized in the following in order to explain the changes needed for adapting the TOF mass analysis.

Trapping experiments are usually performed in a pulsed mode. Primary ions are produced by electron bombardment in an external storage ion source[11] where they are stored and undergo many collisions in order to prepare ions in their electronic and vibrational ground state. For filling the trap, a

train of ions extracted from the source is mass selected in a quadrupole filter. The proper time sequence of opening the source and closing the trap has to be used together with soft injection, i.e., the ions are typically decelerated into the trap to energies below 50 meV in order to prevent collision induced excitation or dissociation. Interaction with a buffer gas couples finally the ion temperature to that of the surrounding walls. Two phases of a rf voltage applied to the trap electrodes give rise to the storing potential which confines the ion cloud in radial direction. This potential is dominated by a field free area around the axis of the trap where ions travel in straight lines at thermal velocities and a steep wall close to the electrodes where the ions are simply reflected without a strong interference with the driving field. Therefore, in such a trap, ion molecule collisions can be studied in nearly thermal conditions (for details see Ref. 11). In order to reach low temperatures, traps are connected to a liquid nitrogen reservoir or mounted onto a closed cycle refrigerator.

The ions can be stored for times varying from microseconds to minutes. In practice, the storage time is limited by residual gas components which deplete the number of primary ions due to parasitic reactions. Therefore the cleanness of the vacuum system is mandatory for reaching high sensitivity. During storage the ions can interact with the neutral reactant or buffer gas. In recent developments the trap can be intersected axially with a beam of condensable molecules, radicals, or atoms. In addition, laser beams can be utilized to excite the trapped ions. After a selectable storage time the potential of the exit electrode is lowered, usually to a potential at which the ions leave the trap rather slowly, often in several tens of microseconds. Under certain conditions, e.g., caused by potential distortions, emptying the trap can take much longer. In this case additional steering electrodes, surrounding the trap, can be used to accelerate the ejection process. The extracted ions are mass selected in a quadrupole mass filter and detected with a conventional ion counting detector where they are registered with almost unit efficiency. Typically, only a few hundred to some thousand parent ions are used in order to avoid space charge effects. Therefore, the measuring procedure *injection/storage and reaction/analysis* has to be repeated rather often, especially because in a QMS only one mass is being detected each time.

In this work a ring electrode trap, RET, has been used for storing the ions. A short description of this special device can be found in Refs. 11 and 22. For interfacing this trap to a TOF-MS, some features of the electrode arrangements have to be considered in more detail. The RET is drawn schematically in Fig. 1. It consists of 20 axially symmetric ring electrodes (inner radius $r_0 = 5$ mm, thickness 1 mm, spacing 1 mm) alternately connected to two opposing metal bars. They are connected by a cryocooled (liquid N_2) tube forming a coil, having an inductance L. Together with the capacitance C of the ring electrodes and an externally connected capacitance, it forms an LC circuit at a resonance frequency of 6.7 MHz. The oscillation is induced by the indicated coupling coil connected to a rf generator. The dc potential of the trap is supplied to the center point of the coil and is kept near to the ground potential of the apparatus. The
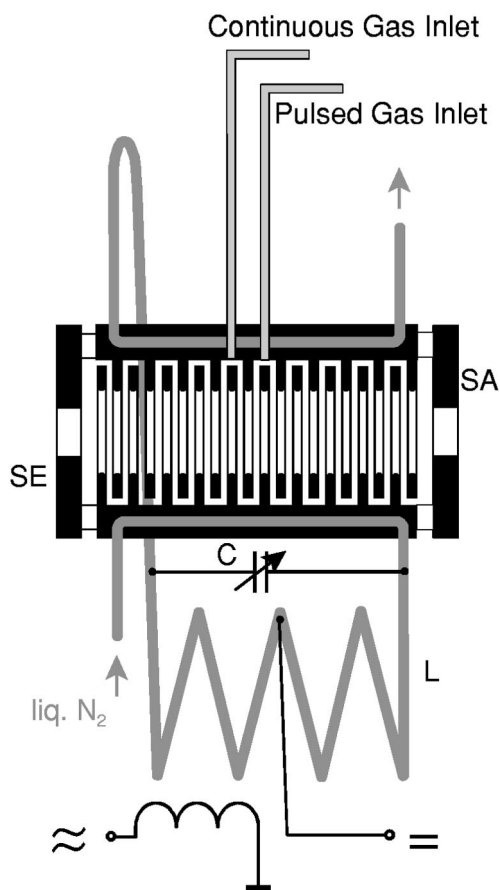
FIG. 1. Schematic drawing of the ring electrode trap (RET). The effective potential confines the ions radially and the positive dc potential of the end electrodes (SE,SA) axially. Ions are injected by a pulse to the entrance electrode SE and, similarly, are extracted using the exit electrode SA. Typically, up to 10^6 ions can be stored for periods ranging from microseconds to minutes. Number densities of neutrals from the continuous gas inlet range from 10^{11} to 10^{13} cm^{-3}. Using the pulsed gas inlet peak densities above 10^{15} cm^{-3} can be achieved during a few ms.
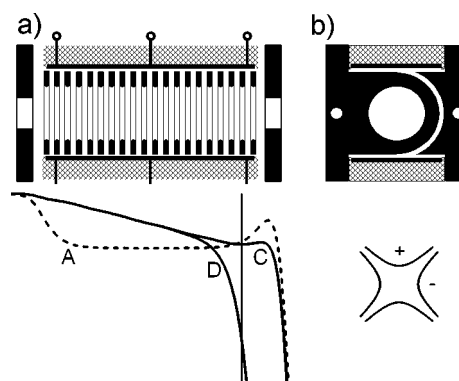

FIG. 2. Schematic drawing of the RET and potentials inside the trap. (a) Axial cut of the RET. By rotating the trap by 90° with respect to Fig. 1, the correction electrodes appear at the top and bottom of the graph. Hatched bars indicate the ceramics body and the solid line the resistive coating. The bottom panel shows the potentials along the trap axis during time intervals A (regular trapping), C (prior to extraction), and D (during the extraction) (see Fig. 3). The thin vertical line indicates the place where the ions are assembling. (b) Cut in a radial plane of the trap. Lower part: quadrupolar field induced by the correction electrodes. The signs + and − indicate the potential difference with respect to the trap axis during the compression phase.

potential of the gate electrodes (SE, SA, 6 mm inner diameter), see later, is referenced to this dc potential.

From Fig. 1 it is apparent that this design is rather simple in comparison to multipole traps[21] where special materials (isolating electrically and conducting thermally) are used. Here only eight ceramic spacers (see Fig. 1) are used to hold all electrodes together. Note that the tubing of the coil serves as supply for the rf voltage as well as for the cooling liquid. In this way the trap can be operated at liquid nitrogen temperature but elevated temperatures (up to 500 °C) are also allowed. These features make the RET especially suitable for studying interactions of stored ions with beams of condensing material, e.g., atomic beams of metal or carbon, a molecular beam of water, etc. The minor drawback of the RET is that potential distortions on the electrodes due to surface charging can have larger effects compared to multipole designs. In order to minimize such effects the stainless steel electrodes have been coated with a thin film of graphite. Important for the present applications are the two correction electrodes mounted onto the side of the trap as shown in Fig. 2. These electrodes are made of ceramics covered with a carbon film having a resistance of about 700 kΩ. They are connected in parallel on each end, and a third contact is in the middle. Application of suitable voltages to these three contacts leads to a potential gradient along the trap axis. In this way the position of the ion cloud in the trap can be controlled.

In the present experiment no external ion source was used but primary ions were produced directly inside the RET via electron bombardment of a suitable precursor gas. For this purpose a miniature electron bombardment evaporation source[23] was modified to produce a pulsed electron beam which was injected into the trap on axis. Ions with kinetic energies below the trapping potential and fulfilling the adiabaticity criterion $\eta < 0.3$ are safely stored.[11] A typical measuring cycle consists of *ion creation/storage and reaction/ extraction and TOF analysis.* Because of the special extraction sequence which is needed for the TOF analysis and which will be described in the following, the shortest storage time was about 200 ms.

The details of the timing sequence which has been utilized to localize the ions at the end of the trap and to extract them all at once, are illustrated in Fig. 3. The *storage and reaction* period (A) already ends almost 50 ms before the trap is actually opened ($t = t_{\text{ext}}$). During period (B), a compression voltage (280 V) applied to the left end of the correction electrodes is switched on gently. The right end is kept at the dc potential of the RET in order to minimize the effects of the transverse field indicated in Fig. 2(b). The voltage applied to the correction electrodes is about 500 times larger than the resulting potential shift in the inside. The time constant of the rising edge of the compression voltage (~4 ms) is defined by a corresponding RC circuit. The slight potential slope accelerates the ions towards the exit electrode. Due to collisions with neutral buffer gas (10^{12}–10^{13} cm^{-3}), the gained kinetic energy is dissipated rather quickly by collisions. Nonetheless the potential of the
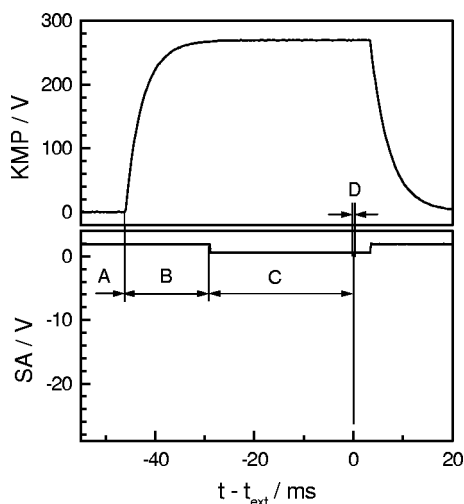
FIG. 3. Ion extraction sequence. Upper panel: temporal evolution of the compression voltage, KMP, applied to the left end of the correction electrodes (see Fig. 2). Lower panel: voltage applied to the exit electrode, SA.

extracted ions are first accelerated to 35 eV followed by a nearly constant electric field created by eight equidistant electrodes (total length 8 cm). The following three electrodes (9–11) form an einzel lens and the electrode system (12–15) is used for steering the beam of ions in the x and y direction. Then the ions, with a kinetic energy of 150 eV, enter the field free region which is made of two tubings. The latter one extends close to the ion detector, consisting of two conventional microchannel plates (MCPs) in chevron arrangement. Here the ions are accelerated to typically 2.5 keV in order to achieve high detection efficiency.

Time focusing leads to instantaneous count rates which are too high to be handled, even with today's fast electronics. Therefore an analog detection scheme has been employed in the current setup. The signal from the electron collector is first amplified ten times using a fast preamplifier. One output is connected to a discriminator[25] for ion counting, when possible. The second output is connected to a digital storage oscilloscope[26] for analog recording of the signal. The data acquisition is triggered by the extraction pulse. Typically the analog signal is digitized into 10 ns bins and averaged over a number of extraction events. The high sampling rate of the oscilloscope, oversampling, allows us to smooth single sweeps for the online signal observation. The transient is transferred to a PC for data processing. Usually, 100 μs of TOF signal are acquired which corresponds to a maximum m/q of about 450 u/e.

For testing and characterizing the performance of the setup, various experiments with CO and He buffer gas have been performed. As a typical result, Fig. 5 shows a TOF mass spectrum of an ion cloud, extracted after a storage time of several seconds. Besides $(CO)_n^+$ clusters some ions are present, produced directly from background gas or by chemical reactions. In order to derive absolute values for the number of ions from such data, first the base line must be subtracted. The offset, which is primarily due to a dc preamplifier signal, is determined from regions where no ions are present. In this example, the interval between 2 and 14 μs has been evaluated because no ions lighter than C^+, 12 u, are stored at the trapping conditions used. The first 2 μs must be excluded because they are influenced by the fast rise of the ion extraction pulse. Absolute numbers of ions are calculated by integrating the signal over suitable time inter-
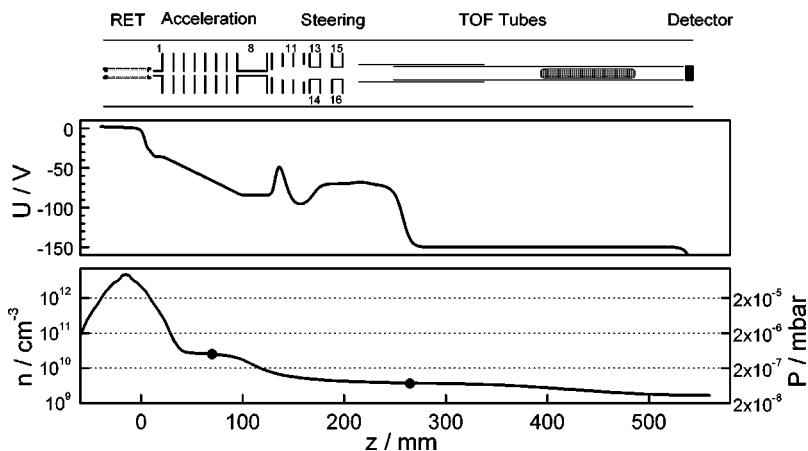
exit electrode must be sufficiently high during the compression phase in order to avoid ion loss. Later the exit electrode is lowered from 2 to 0.7 V with respect to the dc voltage applied to the trap. These values have been chosen comparably high in order to maintain safe trapping conditions in view of space charge effects due to the compression of the ion cloud. During the following 30 ms, thermalizing collisions lead to localization of all ions close to the exit electrode. Finally, in phase (D), a pulse having an amplitude of −26 V, a slew rate of 600 V/μs, and a duration of 100 μs is applied to SA. The potential gradient at the nominal start position is 1.6 V/mm as calculated by SIMION 6.0.[24]

After leaving the trap, the ions enter the TOF device. The upper part of Fig. 4 shows the electrode arrangement of the whole system consisting of the RET (left), a set of acceleration and steering electrodes, the TOF tubing and detector. Its overall length, from the calculated starting point in the trap to the detector, is 57 cm. Since the trap is operated near ground, all the other electrodes have to float at higher voltages contrary to most TOF-MS designs. The axial potential shown in the middle panel of Fig. 4 has been calculated using SIMION 6.0 (grid size 2440×200 points). The typical voltages applied to the electrodes have been utilized as boundary conditions. As can be seen from this graph, the

FIG. 4. Characterization of the Trap-TOF-MS instrument. Upper panel: schematic electrode arrangement along the axis, z. The scale at the bottom is valid for all three panels. Middle panel: simulation of the potential, U, along the axis assuming rotationally symmetric electrode arrangements (extraction moment). Lower panel: number density of neutrals, n and pressure, P in the RET along the TOF path.
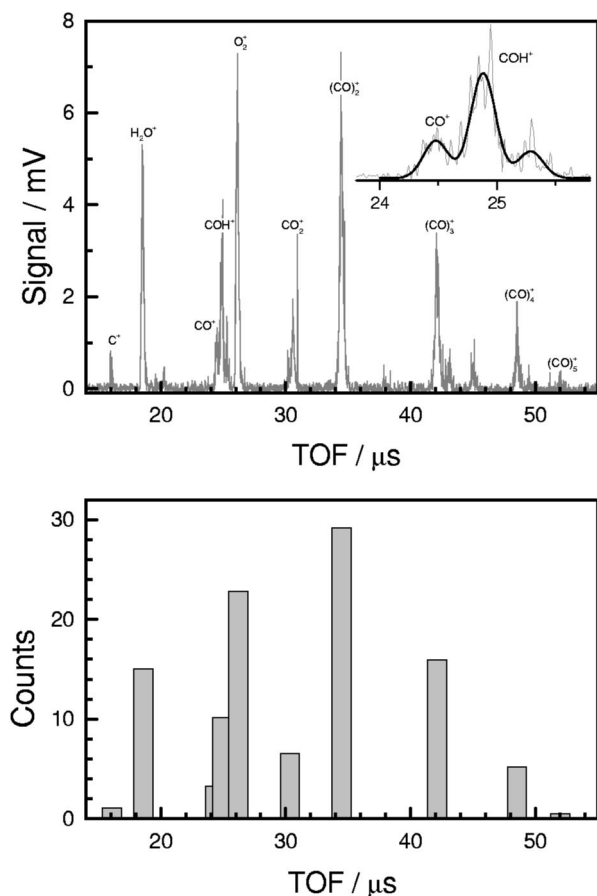
FIG. 5. TOF spectrum of the ions after 4.5 s storage time. Experimental conditions: He buffer gas density 5×10^{12} cm^{-3}, CO reactant gas with a peak density of approximately 5×10^{14} cm^{-3}. Upper panel: average signal of 20 extractions with a corrected base line. The inset shows the masses 28, 29, and 30 u together with Gaussians, fitted to the signal. Lower panel: total number of ions per mass determined by the calibration procedure.

vals and by using a calibration factor which has been determined to be 0.07 nV s per single ion (for this detector and for CO$^+$ ions). This value is consistent with a MCP amplification factor of 10^6, the 50 Ω load, and a tenfold preamplification. Figure 5(b) shows, for the most abundant ions, the result of this very robust evaluation procedure which is especially suitable for processing large sets of spectra. The integral over the full range, i.e., the total number of all detected ions, is extracted directly from the TOF distribution. This number is important additional information for checking charge conservation in the trap and the transmission of the instrument.

Despite keeping all voltages constant during signal sampling, including the extraction potential, a slight temporal change of the base line has been observed. Therefore, in some cases, an alternative local evaluation procedure is preferred, based on fitting suitable functions to the mass peaks. An example of a fit to three neighboring peaks is given in the inset of Fig. 5(a). It is evident that these TOF peaks can be well approximated by 3 Gaussians, having the same width. In general all evaluation methods lead to the same results within the error limits.
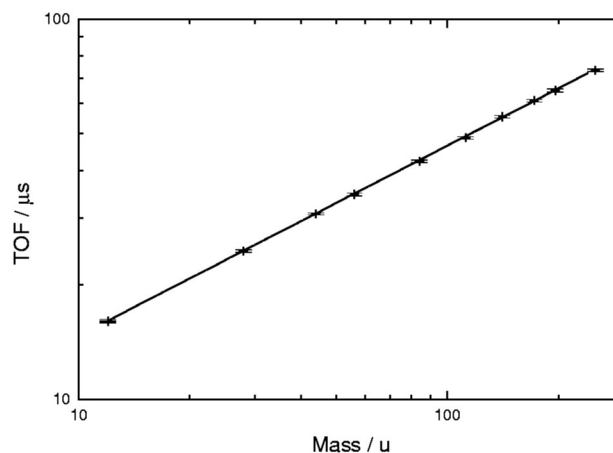

FIG. 6. Calibration of the function TOF vs mass. Observed peaks are fitted to Gaussians and the flight times are derived from their mean positions. The solid line in the log–log presentation is a fit with the result TOF=4.65 μs (mass/u)$^{1/2}$.

III. PERFORMANCE

Important characteristics of the present trap-mass spectrometer combination are calibration of the mass scale, mass range, mass resolution, and dynamical range. In addition, the performance of the present apparatus is affected by problems caused when high gas number densities are used, e.g., for ternary association reactions. The most crucial point of the newly developed device affecting the performance is the compression of the ions prior extraction.

In the ideal case, where all ions fly over the same distance with the same energy, the flight time is proportional to the square root of the mass. In practice the relationship between TOF and mass has to be measured because a rather complicated pulse sequence is used for starting the ions and because of a mass dependent spatial distribution of the ions. The result of such a calibration is presented in Fig. 6. The positions of the mass peaks have been determined by fitting Gaussians as described above. In the log–log presentation, all peak positions fall onto a straight line with the expected slope 1/2. Obviously, there is no significant influence of the rf potential, since the ions start near the axis of the RET. Also, effects caused by the nonideal ion compression (see below) do not play a major role in the arrival time.

The mass resolution can be estimated, for example, from the CO$^+$ and COH$^+$ peaks shown in the inset of Fig. 5(a). Inspection of all peaks reveals that the TOF resolution (full width at half maximum of the corresponding Gaussians) is constant $t/\Delta t \approx 100$ throughout the mass range shown in Fig. 6. The corresponding mass resolution of the device is then given by $m/\Delta m = t/(2\Delta t) \approx 50$. This result is satisfying, considering the opposing requirements of trapping in a large volume and starting at the same time and position. For many applications, this mass resolution is sufficient; however, there are several improvements possible as will be discussed below.

The accessible mass range of the instrument is determined to a small extent by the TOF detection scheme, but predominantly by the trapping conditions. For rf traps there is a limit on the low mass side which can be calculated from
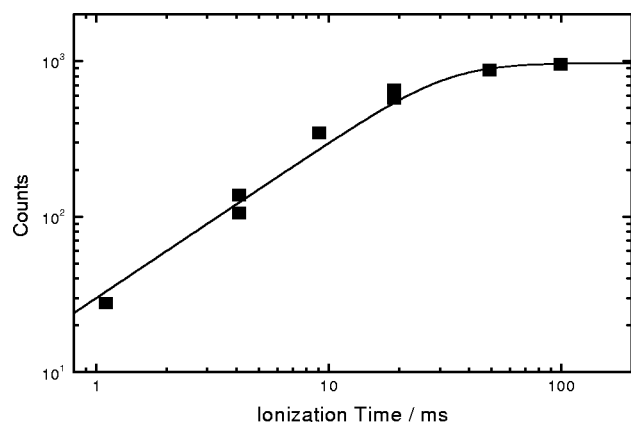
FIG. 7. Total number of detected ions as a function of the duration of electron bombardment. Linear operation is possible up to 700 ions. The saturation for larger intensities is related to space charge limitations during the compression of the ion cloud.

the adiabaticity parameter, and on the high mass side, which is determined by the effective potential. The related formulas can be found in Ref. 11. In the present experiment the RET is operated at a fixed rf voltage, having an amplitude V_0 $= 220$ V and a frequency $\Omega/2\pi = 6.7$ MHz. For a singly charged ion the effective potential is given by V_{eff} $= 0.58$ meV$\cdot$u$/m e^{14.7\cdot\hat{r}}$ and the adiabaticity parameter is η $= 0.041$ u$/m e^{7.17\cdot\hat{r}}$, where $\hat{r} = r/r_0$ is the normalized radius, r_0 the inner radius of a ring electrode, and m the mass. In these formulas the units meV and atomic mass, u, must be used. Allowing for a maximum kinetic energy of 0.1 eV, which is much higher than the most probable value expected for a 80 K thermal ensemble, a mass range of 3–700 u satisfies the safe operating conditions,[11] $\eta_{max} < 0.3$ and $\hat{r}_{max}$ < 0.80. The range actually observed in TOF spectra was 12–250 u. On the low mass side there is no principle problem because He$^+$ ions could also be stored safely; however, there are apparently some difficulties in storing large mass ions. This may be due to the absence of larger clusters in this particular case or it may be related to imperfections in trap geometry or potential distortions. More probable is that the energy gained during the compression phase is larger than 0.1 eV leading to an additional ion loss. In total, the instrument covers in the present version a mass range of about two orders of magnitude which is quite sufficient for studying the growth of $(CO)_n^+$ clusters, $n = 1-9$, as demonstrated below. If one wants to shift the mass range to lower or larger masses, higher or lower driving frequencies for the trap have to be used, respectively.

Another essential criterion for the new instrument is the dynamical range, i.e., the range where the detected signal is strictly proportional to the number of trapped ions. In order to find the limit where saturation effects show up, the signal has been recorded as a function of the number of ions. Figure 7 shows the result of such a measurement. Note that in this figure the signal has been converted into ion counts as described above, and the ion number has been varied by increasing the ionization time. Up to 20 ms the signal increases linearly as expected; however, it starts to level off at a few hundred ions per trap filling and the saturation limit is one thousand ions. It is known from this trap that, under the

present operating conditions, it can hold up to 10^6 ions/cm^3. Also, saturation of the MCP detector and/or the data conversion procedure has been excluded as a reason. Instead, there are several indications that the compression of the trapping volume (about 2 cm^3) by a factor of about 100 leads to space charge loss, limiting the maximum number of ions. The influence of phase space compression and ways to reduce saturation will be discussed in more detail below. On the low intensity side the dynamical range is limited by time width of the mass peak and the noise of the detector, which is typically 1–2 counts/s.

The performance of the present setup is significantly influenced by the fact that the trap is operated at comparably high gas number densities, whereas collision free conditions should prevail in the mass analyzer and detection system. Sufficiently high buffer gas densities for collisional cooling are needed for the phase space compression of the ion cloud for TOF analysis. Especially high densities are required if one wants to study cluster growth via ternary collisions as in the present illustration. In order to reach high number densities in the storage region, the reactant gas is leaked into the trap as indicated in Fig. 1 while pumping the trap is only supplied via the openings formed by the entrance and exit electrode. The resulting pressure profile is displayed in the lower panel of Fig. 4. Inside the trap, the density on axis was measured by a spinning rotor gauge, two points represented by solid circles were measured by ionization gauges. The solid line presents the interpolation of the values on the apparatus axis. Differential pumping is used to separate the trap vacuum chamber from the chamber housing of the TOF detector. In order to allow for enough collisions during ion compression and to limit the number of collisions in the TOF region to a negligible amount, the gas density in the trap must be kept between 5×10^{11} and 5×10^{12} cm^{-3} during the extraction procedure. After leaving the trap the ions are so energetic that collisions lead to their dissociation. In the present setup, changes in the TOF spectra due to collision induced dissociation (CID) become observable for densities inside the trap above 3×10^{13} cm^{-3}.

Most critical for the performance of the instrument presented is the time dependent potential superimposed to the rf trapping field via the external compression electrodes which influences the shape of the cold ion cloud. The spatial distribution of the ions which is finally present at the moment of extraction, is imaged in time and space via the acceleration optics and steering electrodes of the TOF device to the detector. The form of the starting potential is therefore most important not only for the mass resolution of the device but also for the transmission of ions to the detector. The aim of the pulse sequence is to prepare temporal as well as spatial focusing conditions for interfacing with the TOF-MS. The principle of operation which is illustrated in Figs. 2 and 3 has been explained above. However, for a full understanding of the influence of the correction electrodes, the potential distribution perpendicular to the axis also has to be considered. Due to the fact that these electrodes are located only on two sides, see Fig. 2, one obtains a quadrupolar field in the radial plane. Applying a positive potential on the entrance side and leaving the exit side at the trap potential makes this field

weak. The resulting small potential is drawn schematically at the lower part of Fig. 2(b). Here the positive equipotential lines belong to the compression potential of the correction electrode as indicated in the upper part of this figure while, seen from the center of the trap, the ions are attracted to the two sides, marked with a minus sign, where the mounting block of the ring electrodes are. As a result, the ions are not only pushed towards the exit during the compression phase, but they are also pulled into the rf walls. Here they experience a stronger field gradient, i.e., the stability parameter becomes exponentially larger (see formula above). This may cause some loss of ions. In order to avoid this the adiabaticity condition, $\eta < 0.3$, also has to be fulfilled during the compression phase. A transverse potential gradient can be easily avoided by using rotationally symmetric electrode arrangements. A more thorough discussion of an improved setup will be given in the concluding paragraph. Next, the use of the present instrument is demonstrated for a study of cluster growth.

IV. CLUSTER FORMATION

For illustrating the features of the newly developed RET-TOF-MS apparatus it has been used for studying the growth of $(CO)_n^+$ clusters. The dynamics of formation of molecular clusters is an interesting field of ion chemistry because the binding energies are several hundred meV for adding the first molecules to the ion and reach the heat of evaporation of the liquid, typically only a few meV, for larger clusters. This change of bonding can be found in many systems and has been studied in detail during the last 25 years.[27]

In the present example CO^+ primary ions have been formed by pulsed electron bombardment of the reactant gas CO, directly during the first few milliseconds in the liquid nitrogen temperature cooled trap. After different storage times varying from 50 ms up to 9.55 s in steps of 0.5 s, TOF spectra have been taken. The number of ions, extracted from these spectra as described above and corrected for discrimination, are plotted as a function of storage time in Fig. 8. It is obvious that the mass composition undergoes a fast temporal change by the growth of clusters. For reaching clusters up to $n = 4$, a number density of neutrals, $[CO] = 1.2 \times 10^{13}$ cm^{-3}, has been chosen. This value is slightly higher than the optimum for the TOF analysis discussed above. From the semilogarithmic presentation it can be seen that the primary CO^+ ions disappear exponentially by forming $(CO)_2^+$ ions via the ternary association reaction

$$(CO)_n^+ + 2CO \rightarrow (CO)_{n+1}^+ + CO \tag{1}$$
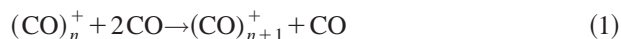
for $n = 1$. Due to discrimination of low mass ions, the signal of CO^+ ions is hard to detect at storage times larger than 4 s. As soon as a significant amount of $(CO)_2^+$ is formed ($t \sim 1$ s), the next step of association, $n = 2$, is observed. At about 4 s a stationary state for dimers is reached; the rates of formation and loss due to further growth are equal. Similarly the production of $(CO)_4^+$ starts significantly when enough $(CO)_3^+$ ions are formed ($t \sim 4$ s). From the rates of changes of the particular clusters, rate coefficients for the growth processes gi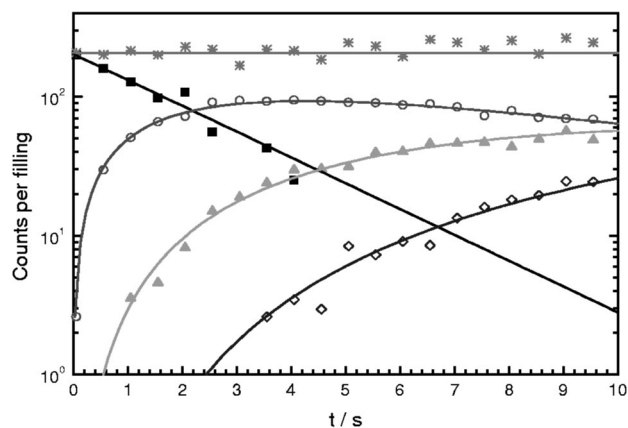ven by Eq. (1) have been determined. The solid lines in Fig. 8 are solutions of a set of master equations accounting for ternary association and, in part, for dissociation. The resulting values for ternary rate coefficients are 2.2×10^{-27}, 8×10^{-28}, and 6×10^{-28} cm^6 s^{-1} for the first three steps represented by Eq. (1). Although not being the subject of this article, they are in good accord with measurements performed in the 22PT with a conventional QMS as an analyzer.[28]

Analyzing the sum of all ions at each storage time, a strong discrimination of small mass ions and a moderate discrimination of higher mass ions has been found. As discussed above, this discrimination is predominantly due to the compression and extraction process and partly due to the fact that the experiment has been performed at too high number densities; however, in this test the major aim was to illustrate that the simultaneous monitoring of all ions allows one to quantify such loss processes, because the rate of change of a parent ion, e.g., CO^+ is related to the rate of change of the daughter ion, $(CO)_2^+$ in this case. For example, $(CO)_5^+$ is discriminated by a factor of 4 relative to $(CO)_2^+$. Using a higher rf frequency would reduce this problem. Another difficulty in the present trapping experiment is that other ions such as C^+, COH^+, O_2^+, and CO_2^+ also play a role. They are not included in Fig. 8, but they all appear in the TOF mass spectrum and can be taken into account for completely describing the kinetics.

For testing the high mass limit of the trap, it is necessary to initially store larger clusters and follow their temporal evolution. In previous studies on hydrogen cluster ions[13,14] it has been demonstrated to be difficult to inject ionic clusters from an external source into rf traps because they are so fragile that they easily fragment before being thermalized. An alternative approach used in the present work is to produce large clusters directly in the trap using a target density way above the limit for CID discussed above, however, only during a short time. In the present configuration (pumping
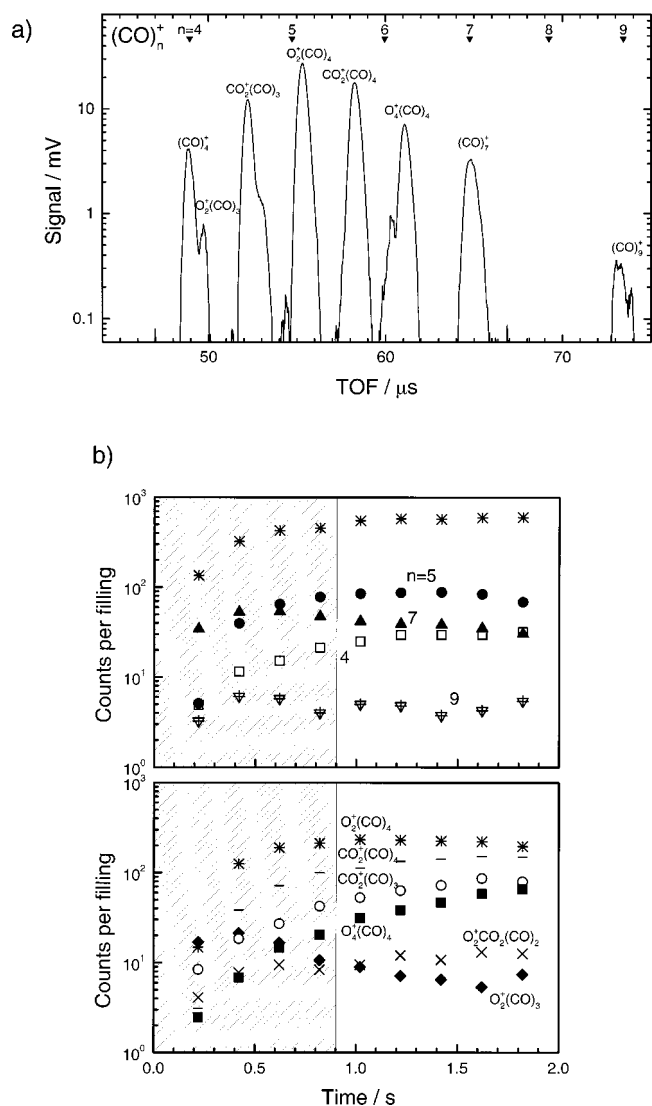

FIG. 8. Growth of CO cluster ions in the RET at $T = 80$ K. The temporal evolution of $(CO)_n^+$ for $n = 1-4$ is marked by the symbols ■, ○, ▲, and ◇ (time interval 10 s). The sum is marked by *. The absolute number of ions has been obtained from calibrated TOF distributions. Data points represent an average over 20 trap fillings. The temporal development shows the exponential decay of CO^+ and sequential formation of $(CO)_2^+$, $(CO)_3^+$, and $(CO)_4^+$ ions in ternary collisions with CO. Solid lines represent the result of a simulation of the kinetics.

FIG. 9. Growth of larger clusters. (a) Averaged TOF spectrum at 1.5 s after the gas pulse. Primary ions are converted to larger clusters $(CO)_n^+$, $n = 4-9$ and to other products of the form $C_xO_y^+$. (b) Ion counts extracted from the TOF spectra at nine times between 0.22 and 1.82 s. Extracting ions from the trap during the high density period of the CO pulse (hatched area) leads to false ion numbers due to ion loss. After about 1 s the gas density is low enough that temporal evolution of larger CO cluster ions (upper panel) and for the $C_xO_y^+$ ions (lower panel) can be followed quantitatively.

speed, geometry) CO number densities of several $10^{15}\,cm^{-3}$ have been reached in the RET during the pulse with a decay time constant of tens of ms.[29] Since cluster production is a ternary process, the growth rate is greatly enhanced during the high density pulse.

In detail, the experiment has been performed as follows. First He^+ primary ions have been produced by ionizing a stationary helium background gas ($\sim 2\times10^{12}\,cm^{-3}$) with a 10 ms electron pulse. Then the trap was filled with CO, using ten pulses from a piezo valve oscillating at a repetition rate of 2 kHz. The electron pulse and the intense gas pulse were well separated in order to avoid arcing or discharges. The initial CO^+ ions grow very rapidly up to $(CO)_9^+$ as can be seen from Fig. 9(a). This mass spectrum has been acquired 1.5 s after the gas pulse. Due to the presence of some residual gas, e.g., O_2, other products of the general form $C_xO_y^+$

are produced as well due to association reactions during the gas pulse or via other chemical reactions.

The temporal evolution of clusters with $n > 4$ is shown in Fig. 9(b). Due to the high density pulse, extraction without discrimination is not possible at times indicated by the hatched area. After 1 s, when the density outside the trap drops below $\sim 5\times10^{10}\,cm^{-3}$, the sum of detected ions becomes constant. During the first second, there is an obvious growth of the number of clusters; however, ion loss during compression and extraction and also CID, apparent in TOF spectra, leads to detected ion numbers which are not at all representative of the actual growth processes occurring inside the trap. After this first time, however, the cluster size distribution is in good accord with an estimate based on the abovementioned ternary rate coefficients and a reasonable temporal and spatial density profile.

A detailed discussion of the interesting kinetics observed during these experimental tests will be published elsewhere;[30] here only a few obvious facts are briefly mentioned. In the mass spectrum given in Fig. 9(a), no $(CO)_8^+$ clusters are detected. One plausible explanation is that the transition from $n = 8$ to 9 is much faster than from 7 to 8. This is indicative for $(CO)_7^+$ being an especially stable configuration. A related observation is the slow decay of $(CO)_7^+$ seen in Fig. 9(b). With the limited statistics of this measurement and with the absence of $(CO)_8^+$, no clear correlation to another cluster channel can be found. Clear correlations, however, are seen between the decrease of $O_2^+(CO)_3$ and $O_2^+(CO)_4$ and the increases of $O_2^+(CO)_5$ [Fig. 9(b)]. Also $CO_2^+(CO)_3$, $CO_2^+(CO)_4$, and $O_4^+(CO)_4$ show a significant increase, although in these cases no decreasing counterpart has been identified. Some of the observations may be induced by intracluster isomerization known from the literature.[31] The existence of clusters such as $CO_2^+(CO)_n$ or $O_2^+(CO)_n$ in addition to $CO^+(CO)_n$ has been found before.[32] Maybe the present observations give hints to intracluster chemical reactions. However, it is also clear that better vacuum conditions are needed for a more detailed analysis. Corresponding work is in progress.

V. NEXT IMPROVEMENTS

In the present work, a RET trap has been combined with a TOF mass spectrometer for following the changes of ion composition simultaneously for a wide range of masses. In order to match spatial distribution of the trapped ions which extends in multipole or ring electrode traps usually over several cm^3 to the TOF-MS device, the ions were compressed by a special sequence of time dependent voltages applied to various electrodes. In addition, inelastic collisions were used for reducing the phase space. In the present setup, a mass resolution of 50 has been obtained. Using a reflectron instead of the linear flight path this value certainly can be improved. Other improvements of the instrument are also obvious. For example, the gas densities used during the reaction period and the buffer gas density needed for the compression phase must be controlled independently. This can be achieved by installing additional pulsed gas inlets or using molecular beams. Also ms-fast shutters should be installed, both for

closing the trap on the two ends and for separating the trapping region from the vacuum chamber containing the analytical instruments.

There are also more suitable electrode arrangements for compression of the ion cloud; for sure one has to avoid any transverse acceleration. Also the geometry of the region where the ions are prepared for the start into the TOF path can be probably improved; a rf quadrupole-type field distribution is certainly better than the electrodes used in this first test. However, there are some fundamental questions which should be discussed if one intends to design a new instrument from scratch for combining low field ion traps and a TOF device. In principle one has to find the best solution for transforming the initial phase space volume, which is extremely small for low temperature multipole or ring electrode traps, to the acceptance of a suitable TOF detector.

In a vastly different approach one should try to avoid ion compression, especially because of space charge effects. Therefore it may be better, instead of trying to assemble a larger number of ions in a small region, to extract them from the whole storage volume by using suitable starting conditions. This may be achieved in a special ring electrode trap where each ring can be supplied with an individual dc potential. In the case of the 22PT used in our laboratory, the set of five mounted correction ring electrodes can be used to superimpose a radially symmetric acceleration field in axial direction. This in combination with a large position and time sensitive detector may lead to a much better performance. In summary, however, it should be emphasized that the solution presented in this article is already well suited to study processes where high sensitivity and a wide mass range are required. One related project going on in our laboratory is the growth of carbon clusters, an experiment where stored C_n^+ ions collect C atoms from a low density carbon beam. Other interesting experiments which can make use of the space focusing properties of the present setup are possible, e.g., IR laser fragmentation of mass selected large cluster ions in a reflectron arrangement.

ACKNOWLEDGMENTS

[1] W. C. Wiley and I. H. McLaren, Rev. Sci. Instrum. **26**, 1150 (1955).
[2] M. Guilhaus, V. Mlynski, and D. Selby, Rapid Commun. Mass Spectrom. **11**, 951 (1997).
[3] J. M. Campbell, B. A. Collings, and D. J. Douglas, Rapid Commun. Mass Spectrom. **12**, 1463 (1998).
[4] T. Bergmann and T. P. Martin, Int. J. Mass Spectrom. Ion Processes **131**, 21 (1994).
[5] B. Moore and M. David Lunney, The Paul Trap as a Collection Device, in *Practical Aspects of Ion Trap Spectrometry*, edited by R. E. March and J. F. J. Todd (Chemical Rubber, Boca Raton, FL, 1995), Vol. II.
[6] G. Sanzone, Rev. Sci. Instrum. **41**, 741 (1970).
[7] V. I. Karataev, B. A. Mamyrin, and D. V. Shmikk, Sov. Phys. Tech. Phys. **16**, 1177 (1972).
[8] H. Wollnik and M. Przewloka, Int. J. Mass Spectrom. Ion Processes **96**, 267 (1990).
[9] G. R. Kinsel, J. M. Grundwuermer, and J. Grotemeyer, J. Am. Soc. Mass Spectrom. **4**, 2 (1993).
[10] G. Niedner-Schatteburg and V. E. Bondybey, Chem. Rev. **100**, 4059 (2000).
[11] D. Gerlich, in *State-Selected and State-to-State Ion-Molecule Reaction Dynamics, Part 1*, Advances in Chemical Physics, edited by C.-Y. Ng and M. Baer (Wiley Interscience, New York, 1992), Vol. LXXXII, p. 1.
[12] D. Gerlich and S. Horning, Chem. Rev. **92**, 1509 (1992).
[13] W. Paul, B. Lücke, S. Schlemmer, and D. Gerlich, Int. J. Mass Spectrom. Ion Processes **149**, 373 (1995).
[14] W. Paul, S. Schlemmer, and D. Gerlich, Chem. Phys. **209**, 265 (1996).
[15] S. Schlemmer, T. Kuhn, E. Lescop, and D. Gerlich, Int. J. Mass Spectrom. Ion Processes **185–187**, 589 (1999).
[16] S. Schlemmer, E. Lescop, J. von Richthofen, and D. Gerlich, J. Chem. Phys. (submitted).
[17] S. M. Michael, M. Chien, and D. M. Lubman, Rev. Sci. Instrum. **63**, 4277 (1992).
[18] N. Zhang, Y. Matsuo, and M. Takami, Chem. Phys. Lett. **244**, 133 (1995).
[19] K. P. Aicher, M. Müller, U. Wilhelm, and J. Grotemeyer, Eur. Mass Spectrom. **1**, 331 (1995).
[20] A. N. Krutchinsky, A. V. Loboda, V. L. Spicer, R. Dworschak, W. Ens, and K. G. Standing, Rapid Commun. Mass Spectrom. **12**, 508 (1998).
[21] D. Gerlich, Phys. Scr., T **95**, 256 (1995).
[22] D. Gerlich and G. Kaefer, Ap. J. **347**, 849 (1989).
[23] V. Nehasil, K. Mašek, O. Moreau, and V. Matolín, Czech. J. Phys. **47**, 261 (1997).
[24] SIMION three-dimensional Version 6.0, Idaho National Engineering Laboratory, 1995.
[25] Philips Scientific, Model 6904, 300 MHz discriminator.
[26] Digital oscilloscope, LeCroy, LT342.
[27] R. G. Keesee and A. W. Castleman, Jr., J. Phys. Chem. Ref. Data **15**, 1009 (1986).
[28] A. Luca, Ph.D. thesis, February 2001.
[29] W. Paul, D. Gerlich, IX International Symposium on Atomic, Molecular Cluster, Ion, and Surface Physics (SASP), Maria-Alm, Austria, 1994.
[30] A. Luca, S. Schlemmer, J. Glosík, and D. Gerlich, J. Chem. Phys. (submitted).
[31] K. Hiraoka, T. Mori, and S. Yamabe, J. Chem. Phys. **94**, 2697 (1991).
[32] M. Meot-Ner and F. H. Field, J. Chem. Phys. **61**, 3742 (1974).